Influence of Proteins on the Hydrothermal Gasification and Liquefaction of Biomass. 2. Model Compounds

Andrea Kruse,* Palanikumar Maniam, and Franziska Spieler

Institute for Technical Chemistry CPV, Forschungszentrum Karlsruhe, P.O. Box 3640, 76021 Karlsruhe, Germany

The hydrothermal gasification is a promising process to produce hydrogen from biomass with high water content. In a lot of cases, this biomass may contain proteins, for example, in residues from the food industry or sewage sludge. In Part I of this serial, experiments on hydrothermal gasification of protein containing biomass (zoo mass) have been reported. This biomass produces lower gas yields than biomass originating exclusively from plants (phyto mass). To understand these findings, experiments with model compounds are necessary. Here, such experiments with model compounds in a tubular and a batch reactor are described. The model system for the phyto mass is glucose with a potassium salt, and the model system for the zoo mass is glucose, potassium salt, and the amino acid alanine. The model systems show a lower gas yield in the presence of alanine. So the presence of alanine in the model system has a similar effect to the presence of proteins in biomass. Additionally, the gas composition and the concentration of selected key compounds are slightly changed by alanine addition. Likely, consecutive products of carbohydrate and protein degradation react with each other. In such Maillard reactions, free radical scavengers might be formed, reducing the reaction rate of free radical chain reactions that are highly relevant for gas formation. Therefore, the gas yield is lower in the presence of proteins or amino acids compared with systems without these compounds. In addition, experiments with real biomass in a batch reactor were reported to verify the assumption of Maillard products reducing free radical reactions. As an example, the addition of urea to phyto mass leads to a decrease of the gas yield to a value similar to that found for zoo mass.

Introduction

The use of biomass for future energy and chemicals production is a challenge for research and development. Biomass is a CO_2-neutral and the only carbon containing renewable energy source. Because of the various kinds of biomass, differing in amount, consistency, and chemical composition, appropriate technologies have to be developed for extensive and efficient use. For wet biomass containing large quantities of water up to 90%, hydrothermal gasification appears as a useful conversion technology. Many studies on the degradation of biomass or biomass model compounds in near-critical and supercritical water have been published.[1−52] The experiments were conducted in batch,[1,2,9−13,17,19,20,22,24,25,28−30,34−37,39,41,49−52] semibatch,[18] and continuous reactors.[3−5,7,8,15,16,21,23,24,26,27,30−34,37,38,42−44,46−48] Here, the conversion of model compounds like glucose,[1,3,4,6,23,24,27−31,36−39,50] cellulose,[11−13,15,19,20,22,37,39,42,49−52] lignine,[49,51] and others,[8,16,21,22,36,39,43,45,47,48] as well as chemical waste[2,17,34,44] and biomass,[1,4−7,9,10,18,24−26,30,32,33,35−37,39,41,46,51] were studied. In these studies, the dependence of temperature (sub- and supercritical range), pressure, reaction time, concentration, and catalysts are studied. In addition, different types of feedstock, model compounds, or biomass are compared. In spite of this huge amount of knowledge, the single reactions pathways from the feedstock to the gas are not completely known. The reasons are the high number of compounds involved and the variety of reactions occurring.

As a proven method to handle such a complex reaction like biomass gasification in supercritical water, key compounds were identified.[26,29] These key compounds are intermediates and representative for different reaction pathways (see Scheme 1),

Scheme 1. Simplified Reaction Mechanism for Biomass Degradation

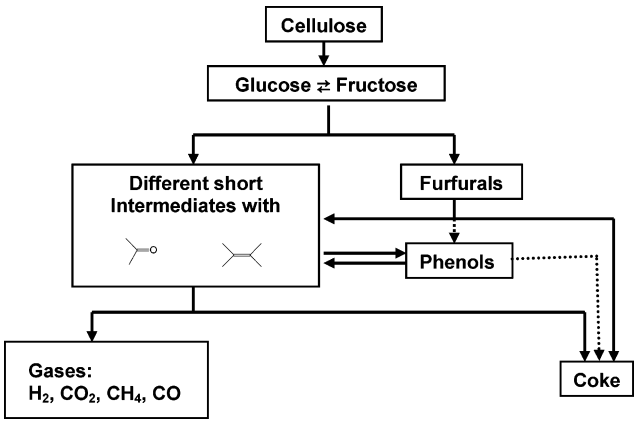

from which a simplified reaction network can be derived. Here "short intermediates" stands for a huge number of compounds with a lower molecular weight than glucose and often with carbonyl groups and C−C double bonds. This reaction network is also valid for glucose as the starting material, if the first step is omitted. The reader should take into consideration that a single key compound usually represents a group of similar components reacting via a certain chemical reaction pathway. Changes in the chemical reaction network are indicated by changes of the concentration of one or more key compounds. The key compounds analyzed here are as follows: glucose, fructose, hydroxymethylfurfural, methylfurfural, furfural, phenol, toluene, cresols, acetic aldehyde, formic aldehyde, formic acid, acetic acid, methanol, ethanol, glycol aldehyde (determined as dimethyldioxane, see below), glycol acid, and others. In addition, sum parameters like DOC (dissolved organic carbon) and the sum of all phenols are determined. The reaction types leading

* Corresponding author. E-mail: Andrea.kruse@itc-cpv.fzk.de. Phone: +49 7247 82 3388. Fax: +49 7247 82 2244.

10.1021/ie061047h CCC: $37.00
Published on Web 12/07/2006

to the diverse key compounds are different. The degradation of cellulose to glucose is a hydrolysis,[53] and the formation of furfurals from fructose is a multiple water elimination.[45] Smaller C2- and C3-compounds, here called "short intermediates", are formed by aldol splitting.[54,55] Gases are mainly formed by free radical degradation apart from CO_2, which is formed by decarboxylation of organic acids and via water gas shift reaction from CO. This means the reaction parameters like temperature and additives may influence the various reaction pathways differently. The key compounds are the links between investigations of model compounds with studies of real biomass, because they can be found in the degradation of both. The simplified reaction mechanism shows the degradation of cellulose, the main constituent of biomass. Other ingredients of biomass are regarded as disturbances of this mechanism. At conditions beyond the critical point of pure water (374 °C, 22.1 MPa), typically ~600 °C and 30 MPa, biomass reacts with water forming hydrogen, carbon dioxide, and methane besides small amounts of carbon monoxide and higher hydrocarbons. The state of the art about biomass gasification is summarized in ref 56. Compared with dry biomass conversion processes, only very small amounts of tar are formed, and at optimized conditions, no char/coke is formed. In other words, the gas yield is much higher and downstream gas cleaning becomes easier. Wet biomass, e.g., residues from the agriculture or food industries, mainly originates from fast-growing plants, which consist of cellulose as well as hemicelluloses and usually a low lignin content, but rather high ash contents, i.e., inorganic compounds. Especially the potassium salt content is usually fairly high. It is known that alkali salts have a significant influence on biomass gasification, leading to higher gas yields by improving the water gas shift reaction.[57] Therefore, a mixture of glucose and alkali salts was found to be a better model system for biomass with its high alkali content. If zoo biomass is considered, the biomass feedstock also contains proteins. The influence of proteins is important, because, for example, sewage sludge and other potential feedstocks for hydrothermal gasification include proteins. Also, the degradation of proteins and amino acids has been studied before, e.g., refs 58−64. The interference of proteins with other ingredients of biomass during biomass gasification has not been investigated before.

In Part I of this series, two different biomass feeds and a glucose solution with K_2CO_3 have been compared in regard to their gasification properties in supercritical water.[65] The experiments were conducted in a continuous stirred tank reactor (CSTR). One biomass originated only from plants (phyto mass) and the other contains also meat (zoo mass). A phyto mass consisting mainly of carrots and potatoes and a protein containing zoo mass consisting of chicken and rice are compared. The gasifications of phyto mass and the aqueous solution of glucose and K_2CO_3 show similar results; those of zoo mass differed significantly, leading to the following:

- a lower gas yield,
- a higher CO content in the gas phase,
- a higher dissolved organic carbon content in the aqueous phase,
- higher phenols content in the aqueous phase,
- strong corrosion never found before in hydrothermal biomass gasification studies with this reactor (Ni-particles are found after the reaction in the effluent), and
- a lower formic acid concentration in the aqueous effluent.

In Part I, it was assumed that consecutive products of protein and carbohydrate degradation react via the Maillard reaction to compounds that are free radical scavengers. The gas formation is mainly a result of free radical reactions; therefore, inhibiting the free radical chain reaction reduces the gas formation and increases the concentration of organic compounds in the aqueous effluent. The strong corrosion observed was assumed to be caused by the sulfur components.[65] To make evident that the presence of proteins causes the gasification yield decrease, experiments with model compounds are necessary. Experiments in a CSTR are sometimes difficult to interpret because of the intensive back-mixing; early consecutive products or the feedstock can react with late consecutive products. The following experiments are, therefore, performed in a tubular and a batch reactor. The reactors show no or low back-mixing effects. As a model compound for proteins, the amino acid alanine was used. Additionally, some experiments with "real" biomass have been conducted to test the transferability of the experimental results. The main goal of these studies with model compounds and biomass is to understand the influence of proteins or amino acids in order to avoid or compensate negative effects. This is important in view of the technical application for hydrothermal biomass gasification because it enlarges the range of application to protein-containing feedstock.

Experimental Section

The *tubular reactor* experiments were carried out in a high-pressure apparatus (Scheme 2) equipped with a feeding line, the tubular reactor, a pressure down let, and a sampling system. This reactor was found to behave mostly like an ideal tubular reactor.[66] The measurements have been conducted at 25 MPa, temperatures of 460−550 °C, and reaction times ranging from ~5 up to 9 s. As feedstocks, an aqueous solution of glucose (only at 500 °C, 2 wt % of glucose monohydrate), glucose with $KHCO_3$ (2 wt % glucose monohydrate and 0.2 wt % $KHCO_3$), and glucose with $KHCO_3$ as well as alanine (additional 0.4 wt % alanine) were used. All chemical were supplied by Merck. The aqueous solution was pumped from a storage vessel; the flow rates were controlled by weighing. The reactor was a stainless steel tube (CrNiMo steel; AISI 316L = EN 1.4435; C < 0.03%, Cr = 17.5%, Ni = 12.5%, Mo = 2.6%), 6 m long with an internal diameter of 2.1 mm, seasoned by several similar experiments conducted earlier. The reactor was heated by a fluidized sand-bath. The temperature along the tube was measured by 16 thermocouples. Six thermocouples were spread over the first 50 cm of the reactor, while the others were spaced over longer distances. The bath temperature was constant within ±2 K. After rapid cooling, the product mixture was expanded to ambient pressure by a back-pressure regulator. Here, phase separation occurs. Liquid samples were collected and analyzed. The amount of gases formed was measured by a wet gasometer, and samples have been collected in sampling tubes.

To conduct extra experiments also with real biomass, a *batch reactor* was used, because plugging would occur in the tubular reactor due to the small diameter. Here, two different biomass feedstocks and glucose solution, with and without additives, were used. One biomass originates from plants only (phyto mass, PM). The other contains meat (zoo mass, ZM). The phyto mass used in the experiments was a finely chopped mixture of carrots and potatoes (baby food by Hipp Company). From a chemical point of view, this biomass nearly exclusively consists of carbohydrates with a chemical composition of $CH_{1.9}O_1N_{0.02}S_{0.001}$. The dry matter (DM) content of the initial biomass is 10.8 wt % (89.2 wt % water content). The ash content amounts to 6.2 g/kg, with a relevant content of potassium of 1.2 g/kg as salt having to be mentioned. The zoo mass consists of a finely chopped mixture of mainly cooked rice and chicken

Scheme 2. Scheme of the Tubular Reactor

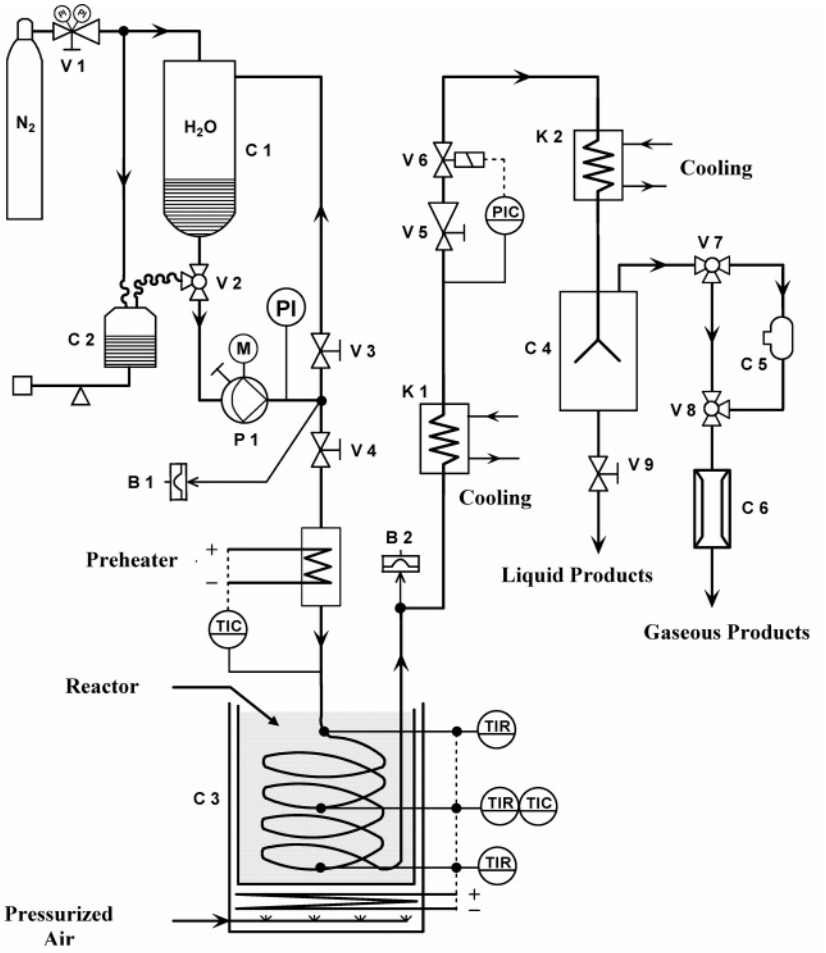

C 1, 2: Storage vessels (C 2 is weighted to control the flow)

V 1-9: Valves (V 5 = micro metering valve and V 6 = piston type air operated valve with regulator for pressure control)

B 1,2: Rupture disks

P 1: Membrane pump

K 1,2: Coolers

C 3: Fluidized sandbath

C 4: Phase separator

C 5: Sampling tube

C 6: Gas flow measurement, later substituted by a wet gasometer

(baby food by Hipp Company). It includes 8.3 wt % proteins, 3.3 wt % fats, and 5.9 wt % different kinds of carbohydrates leading to the chemical composition $CH_{1.8}O_{0.5}N_{0.1}S_{0.005}$. The DM content is 17.6 wt %; the ash content is 16 g/kg. Here, 1.6 g/kg of potassium and 1.4 g/kg of sodium, both as salts, are contained in the zoo mass. The higher nitrogen and sulfur contents of the zoo mass is a result of their proteins content; the high potassium salt content is mainly caused by the rice.

The experiments are carried out in an Inconel 625-lined, tumbling batch autoclave (Figure 1). A photo of the reactor was presented in a previous paper.[67] The autoclave has an internal volume of 1 L and is constructed for a pressure of up to 50 MPa and a temperature of up to 500 °C. The reactor is heated by heating cartridges. Inside the reactor there is a pipe in which three thermocouples are fastened for temperature measurement. The temperature and pressure are controlled by the analogue manometer and thermocouples. Heating rates and the final temperature are adjusted by a temperature controller. The glucose solution or biomass suspension is loaded in the evacuated autoclave by means of valve 1 using a diving tube (Figure 1). After loading, the autoclave is flushed by N_2 to remove all air in the reactor. Then the temperature controller is set to a heating rate of 3 K/min and to the final temperature (500 °C). Mixing was achieved by a motor-driven tumbling movement. After the reactor has reached the final temperature, the experiment is continued for 1 h at 500 °C. After cooling, the amount of gases formed is measured by a gasometer after expansion to ambient pressure. The residual aqueous solution is removed from the autoclave and filtrated, and samples of the gaseous, liquid, and solid phases are analyzed.

To gain some information about corrosion, four additional experiments with zoo mass were performed in which an Inconel

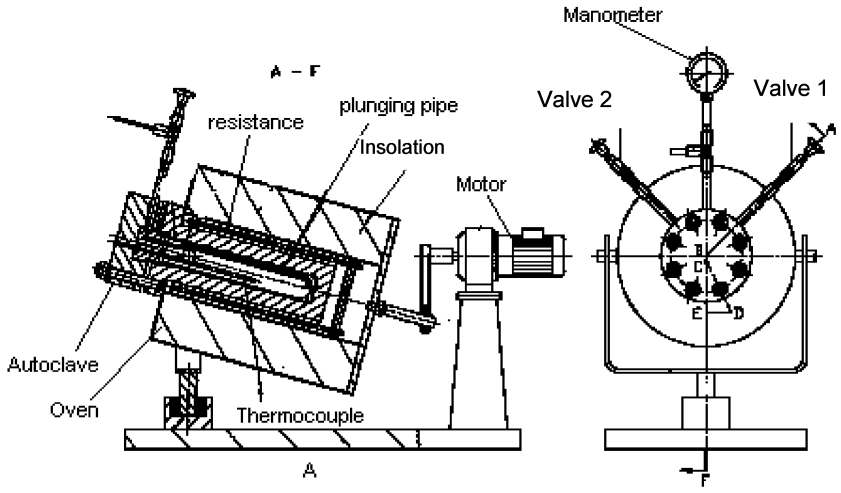

Figure 1. Tumbling batch reactor.

plate (12 × 94 × 2 mm) was put inside the reactor. Before the experiment, one-half of the plate was polished and the other stayed unchanged. In these experiments, always fresh biomass was added to the same Inconel plate. After the gasification, the whole reactor with Inconel plate inside was carefully washed out.

Analysis. *Gas analysis* was carried out by two gas chromatographic procedures. An HP 5889A gas chromatograph (GC) (nitrogen as carrier gas, equipped with a Porapak Q column (80/100 Porapak Q by Supelco, 1.83 m length) and a thermal conductivity detector] was used to determine the hydrogen content. For analysis of all other gases, an HP 6890 GC with column switching and helium as the carrier gas was used. Here, the first column was 80/100 Hayesep Q (2 m long, by Resteck), and the second column was a 60/80 Molesieve 5 Å (4 m long, by Resteck). The two columns as well as a thermal conductivity and a flame ionization detector were connected in series. The second column was bypassed by a six-port valve for analysis of CO_2 and hydrocarbons.

The *liquid products* are analyzed by various methods. The residual dissolved organic carbon content (DOC, obeying German Industrial Standard DIN EN 1484) in the liquid effluent was measured by a commercial TOC/DOC analyzer (Rosemount Dohrmann DC-190). The amounts of different phenols were determined colorimetrically by UV−vis spectrometry (LCK 345/LCK 346, Cadas 200 photometer, by Hach-Lange). The amounts of organic acids and furfurals were measured by liquid chromatography equipped with a high-performance liquid chromatography (HPLC) pump, an Aminex TMHPX-87 H column by Biorad for organic acids, an RP-18 column by Merck for furfurals, and an L-4250 UV−vis detector by Merck.

Solids like corrosion products were formed during the experiments in the batch reactor only and were analyzed by a field emission scanning electron microscope (FE-SEM, LEO Corp., Oberkochem, Germany), combined with an energy-dispersive X−ray analysis system (EDX, Link Isis 300, Oxford Microanalysis Group). For details see refs 68−70.

In all cases, experimental errors, given as error bars in the figures, were estimated from the several-times-repeated measurements. Usually this error was around ±10%. Analytical errors had been much smaller

Results

1. Tubular Reactor Experiments. No plugging, e.g., because of coke formation or salt precipitation, was observed in the experiments reported here.

In Figure 2, the gas yields from the tubular reactor at 500 and 460 °C as a function of the reaction time are shown. The yields are given as gas volume at standard conditions formed. Especially at lower reaction times, the gas yields of the $KHCO_3$ and alanine containing feedstock are smaller than those without alanine. At 500 °C, the lowest yield was achieved for glucose alone. This is a well-known effect of alkali salts on hydrothermal gasification found earlier.[57] The gas yields increase with temperature; this effect appears to be small on first sight. At the constant mass flow given by the experimental setup, the reaction time at higher temperature is much smaller than that at lower temperature. The second reason is that gases are late consecutive products of glucose degradation. So, small differences in early reaction steps can shift the gas formation to higher or lower reaction times. This is not visible in the short reaction time range of the early kinetical regime examined here. So these experiments in the tubular reactor are not suitable to compare different reaction temperature, but the influence of different compositions, at constant temperature, can be well-depicted.

Figure 3 shows the gas composition. Usually the CO content after conversion of pure glucose is high. This is a consequence of the absence of alkali salts catalyzing the water gas shift reaction. CO_2 is the main product of the low-temperature conversion. With an increase of temperature, the hydrogen content increases. In the experiments with alanine, the CO content is higher and the hydrogen content is lower than in the experiments without. This does not mean that more CO is formed in these experiments, because the absolute yield of all gases is lower (see Figure 2). The content of hydrocarbons like

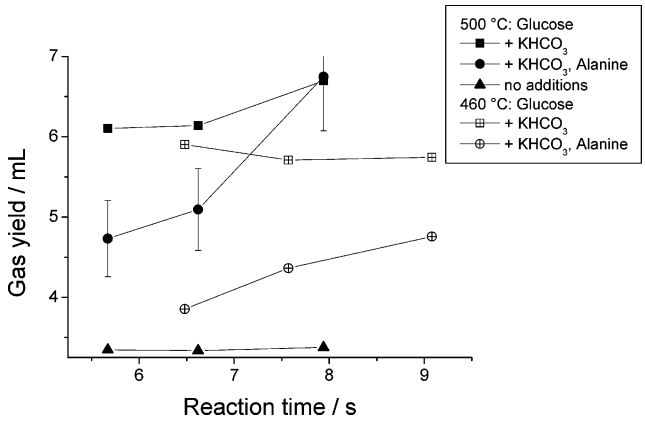

Figure 2. Gas yields at 500 and 460 °C of different glucose solutions as a function of reaction time (2 wt % glucose monohydrate, 0.2 wt % $KHCO_3$, 0.4 wt % alanine, tubular reactor, 25 MPa).

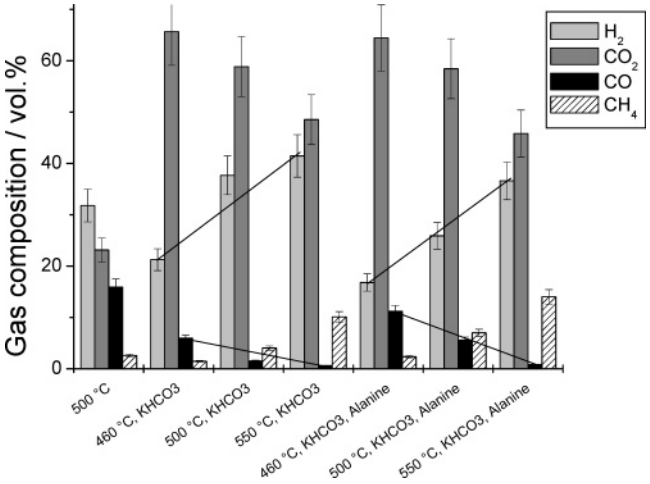

Figure 3. Gas composition at 460, 500, and 550 °C and different compositions (25 MPa, tubular reactor); reaction times: 6.5 s at 460 °C, 5.7 s at 500 °C, and 5 s at 550 °C.

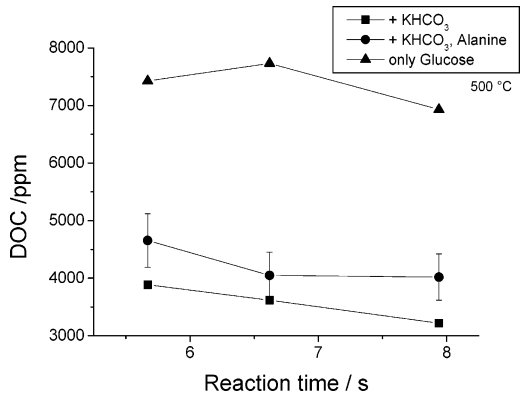

Figure 4. Content of dissolved organic carbon (DOC) as a function of reaction time at 500 °C and 25 MPa in the tubular reactor.

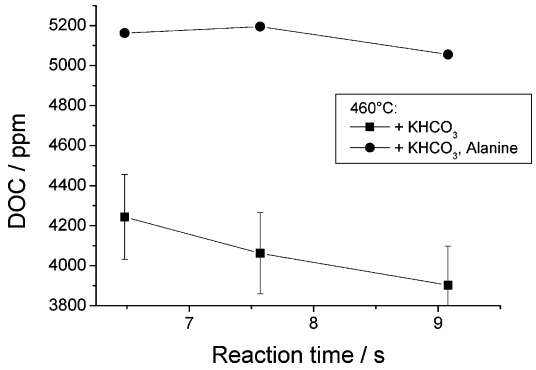

Figure 5. Content of dissolved organic carbon (DOC) as a function of reaction time at 460 °C and 25 MPa in the tubular reactor.

ethane, ethene, propane, propene, and butanes was in a sum below 1 vol %.

A decrease in gas yield should correspond in an increase of dissolved organic carbon (DOC). At 500 °C, the highest DOC content was found after gasification of pure glucose (Figure 4). In all cases, adding alanine to a glucose/$KHCO_3$ mixture increases the DOC content (Figures 4−6). Usually, many different compounds can be identified in the aqueous solution. Here, the focus is on selected key compounds; an important one is hydroxymethylfurfurale (HMF). Its concentration in the aqueous product solution is usually much reduced by the presence of alkali salts. This is also displayed in Figure 7. Adding alanine increases the HMF concentration, but it is still roughly 2 orders of magnitude lower than that without $KHCO_3$.

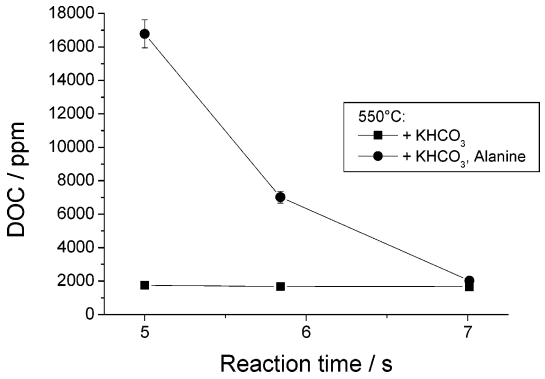

Figure 6. Content of dissolved organic carbon (DOC) as a function of reaction time at 550 °C and 25 MPa in the tubular reactor.

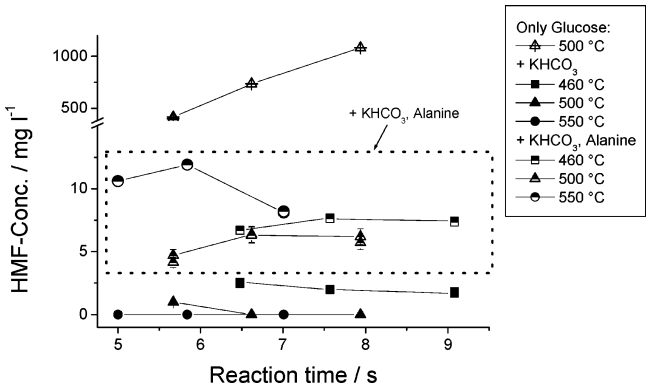

Figure 7. Concentration of HMF at different compositions and three temperatures as a function of reaction time (25 MPa, tubular reactor).

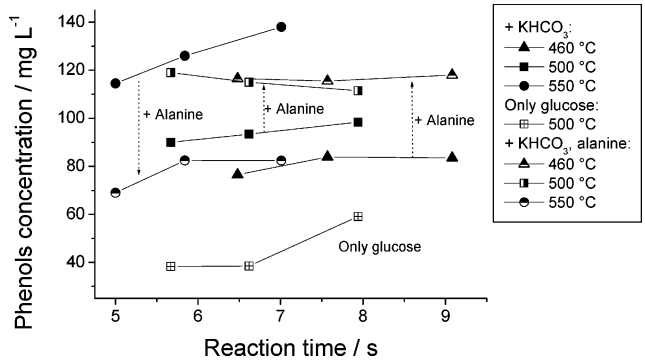

Figure 8. Concentration of phenols at different compositions and three temperatures as a function of reaction time (25 MPa, tubular reactor).

Regarding the concentration of phenols, no uniform tendency concerning the influence of alanine addition was found. From earlier studies, it is known that adding alkali salts increases the phenols concentration and that, at short reaction times, the phenols concentration increases with temperature.[57] Both effects are found here, too: The phenols concentration without $KHCO_3$ addition increases with reaction time from 35 to 55 mg/L (at 500 °C). In all other experiments, the concentration ranges from 70 to 135 mg/L. In the experiments at 550 °C, the phenols concentration decreases in the presence of alanine; at 460 and 500 °C, it is increased. These results are shown in Figure 8.

The concentrations of acetic acid and acetaldehyde decrease slightly with reaction time or remain nearly constant. Table 1 shows the concentration ranges for the different feedstock compositions and reaction temperatures. The concentrations of acetic acid and acetaldehyde are lower without $KHCO_3$ than in its presence. At the same temperature and in the presence of $KHCO_3$, adding alanine increases the concentration of both. On

Table 1. Concentration Ranges of Acetic Acid and Acetaldehyde Summing up the Results from Experiments with Different Reaction Times[a] at Varied Compositions and Temperatures (25 MPa, Tubular Reactor)

reaction condition	acetic acid,[b] mg/L	acetaldehyde,[b] mg/L
500 °C, only glucose	260−651	299−360
550 °C, + $KHCO_3$	22−71	136−374
500 °C, + $KHCO_3$	733−1230	545−822
460 °C, + $KHCO_3$	1200−1360	546−840
550 °C, + $KHCO_3$, alanine	49−103	156−398
500 °C, + $KHCO_3$, alanine	1384−1594	917−1140
460 °C, + $KHCO_3$, alanine	2164−2279	963−1102

[a] Reaction times can be taken from Figure 4 for 500 °C, Figure 5 for 460 °C, and Figure 6 for 550 °C. [b] Experimental error = ±10%.

Table 2. Concentration Ranges of Dimethyldioxane and Glycol Acid at Different Compositions and Reaction Times (25 MPa, 500 °C, Tubular Reactor)[a]

reaction condition	reaction time, s	dimethyldioxane,[b] mg/L	glycol acid,[b] mg/L
only glucose	5.7	5228	736.8
	6.6	5452	795.1
	7.9	4334	673.5
+ $KHCO_3$	5.7	≪detection limit	3
	6.6	≪detection limit	3.2
	7.9	≪detection limit	2.65
+ $KHCO_3$, + alanine	5.7	(0.88)	9.65
	6.6	1.19	9.05
	7.9	2.28	6.15

[a] The detection limit is 0.5−1 mg/L depending on the matrix. [b] Experimental error = ±10%.

the other hand, the addition of alanine has no significant effect on the concentration of formic acid.

Table 2 shows the concentration of dimethyldioxane and glycol acid in the aqueous solution. Dimethyldioxane is in equilibrium with its monomer glycol aldehyde. In aqueous solution and ambient conditions, the equilibrium is on the side of dimethyldioxane. Glycol aldehyde can directly be formed from glucose by aldol splitting.[23,31,55] The concentrations of dimethyldioxane and glycol acid are high if only glucose is in the reactor. Adding $KHCO_3$ leads to a drastic decrease of the dimethyldioxan and glycol acid concentrations. The addition of alanine increases the concentration of these two compounds slightly.

One liquid sample taken after reaction of glucose, $KHCO_3$, and alanine was transported to the company Bruker and was analyzed by ELEXSYS-spectroscopy. The transport took roughly 30 min; despite this rather long time, a small signal of an organic free radical was visible. The signal was too small for identification or further investigations.[71]

2. Batch Reactor Experiments. The same analytic procedure was performed with the samples of the batch experiments. Here, only the results on gas yield and the GC-MS analysis will be presented, because the others do not provide new information.

Figure 9 shows the gas yields achieved with different mixtures. The yield of phyto mass gasification is higher than that of zoo mass gasification. Adding K_2CO_2 increases the yield of zoo mass nearly to the value reached with phyto mass. This effect is found in the CSTR also and was described in Part I.[65] Adding urea to phyto mass drastically decreases the gas yield to an extent lower than that of zoo mass. Urea is used here, because its degradation leads only to CO_2 and ammonia. Adding formaldehyde increases the gas yield of zoo mass to a similar extent as adding K_2CO_3. Combining glucose and K_2CO_3 leads to nearly the gas yield of the phyto mass gasification. The yield of pure glucose or a glucose−alanine mixture is much lower.

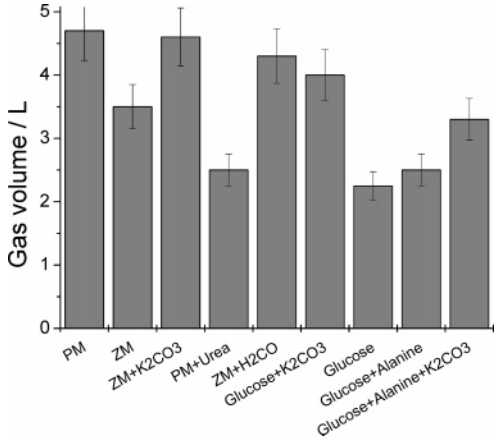

Figure 9. Gas yields after gasification of phyto mass (PM), zoo mass (ZM), and glucose with and without different additions in the batch reactor (dry mass content always 5 wt %, 0.5 wt % K_2CO_3, 1 wt % urea or alanine, 0.5 wt % formaldehyde (H_2CO), heating rate 3 K/min up to 500 °C, 1 h reaction time, ∼30 MPa).

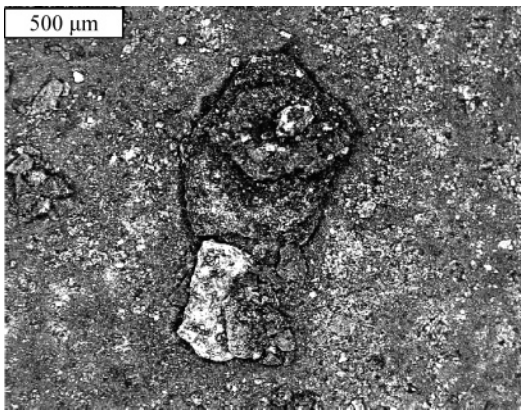

Figure 10. Scanning electron microscope picture of particles forming a thick, black layer on the Inconel plate after reaction.

Combining glucose, alanine, and K_2CO_3 leads to a higher gas yield versus glucose alone but to a lower gas yield versus glucose with K_2CO_3. In fact, it is nearly the same gas yield as that found for the gasification of zoo mass. The K_2CO_3 partially reacts with the CO_2 to form $KHCO_3$ in aqueous solution. This reduces the gas yield in these cases slightly. The effect is neglected here because it is small compared with the effect of the salt on gasification.

Samples of the gasification of glucose in the presence of alanine and K_2CO_3 were analyzed by GC-MS. Besides the usually observed aldehydes, ketones, organic acids, furfurals, phenols, and others (see ref 25), additionally various indoles, pyrroles, and pyridines were found. The last-mentioned compounds can only be formed in the presence of nitrogen containing organic compounds. Additionally, a small peak was identified as a pyrazine derivate, but here this identification is questionable because of the bad peak-to-baseline ratio.

To investigate whether there are corrosion effects visible, additional experiments with zoo mass in the presence of a plate of Inconel 625 (20−23 wt % Cr, 8−10 wt % Mo, 5 wt % Fe, 3.2−4.2% Nb/Ta, and Ni as alloying element) have been conducted. After the reaction, different types of particles were found forming a black layer on the metal surface (see Figure 10). The composition of selected types of particles is shown in Table 3.

In the analysis of the solid particles, hydrogen cannot be detected by the EDX method applied. Despite this, it is likely that the particles Type I are coke and not, for example, formed

Table 3. Composition of Different Particles Shown in Figure 8 (in wt %)

elements	Type I	Type II	Type III	Type IV
C	91.88	34.10	8.63	50.59
N		3.99		14.49
O	5.10	27.54	6.45	8.56
Na			1.60	
Mg		0.25	0.29	
Al		0.65	1.71	0.08
P		0.37	16.44	
S		0.55		7.66
Cl				
K		0.15	0.48	
Ca		0.16	2.05	
Cr	2.5	17.22	13.55	0.04
Fe		1.76	1.84	0.33
Ni		6.96	45.03	17.89
Nb		2.86		
Mo		3.45		

by hydrocarbons. Particles Type II have a relative high content of chromium and a low content of nickel relative to the composition of Inconel. This hints to a corrosion product. Additionally, the particles contain much carbon and oxygen. The oxygen content is higher than could be expected by forming chromium and nickel oxides. Likely a combination of organic solids ("tar") and these metal oxides forms these particles. In the particles of Type III, the phosphorus content is high. The oxygen content is relative low; therefore, the phosphorus is not included as phosphate. Likely some NiP is present in the particle. Type IV particles show the highest sulfur content. Also, the nitrogen content is relative high. Perhaps an organic compound or a mixture of organic compounds of the sum formula $H_XC_8N_2O$ and NiS forms this particle.

No pure nickel particles as reported in Part I were found here. In the experimental error range, all additional experiments with the Inconel plate lead to identical results about composition of gases, liquid phase, and solids as well as gas yield.

Discussion

It is found that adding alanine to a glucose/$KHCO_3$ solution:

- reduces the gas yield,
- increases the percentage of CO in the product gas, and
- increases the DOC content in the aqueous solution.

These effects are also observed for zoo mass compared with phyto mass (Part I of this serial).[65] It is likely that the alanine influences the glucose degradation in the same way as proteins or their consecutive products influence the carbohydrate degradation in the zoo mass. It is assumed in Part I that free radical scavengers are formed via the Maillard reaction (See Figure 11and ref 65). The free radical anion formed is relatively stable. It is not able to start a free radical chain reaction, but it is able to react with other free radicals in a free radical combination reaction. Therefore, the concentration of free radicals and the reaction rate of the free radical chain reaction is reduced.[72,73] Most of the gases are formed by free radical reactions, and therefore, amino acids or proteins reduce the gas formation and increase the DOC content. Pyridines and pyrroles are found to be also free radical scavengers[74] and are formed by similar reactions.

Unfortunately, it was not possible to identify the relatively stable free radical by ELEXSYS-spectroscopy after gasification, but there are clear hints that such reactions occur and are the reason for the lower gas yields. One is the identification of nitrogen containing compounds known to form free radical scavengers. The other is that adding urea reduces the gas formation from phyto mass (see Figure 9). Urea has fewer

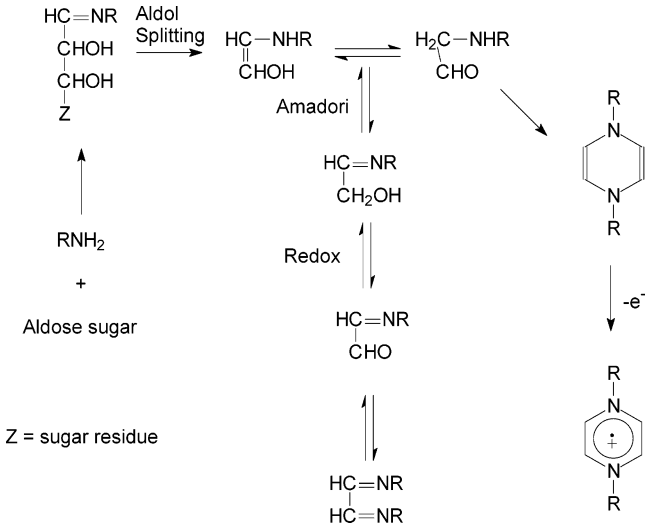

Figure 11. Maillard reaction of amines with sugars (taken from ref 75).

possible reaction pathways than amino acids, but it reacts to ammonia, which is necessary for the reaction shown in Figure 11. In Part I, it is also described that zoo mass degradation leads, at 500 °C, to a higher phenols and a lower formic acid concentration compared with phyto mass. In the experiments with alanine and glucose, the phenols concentration change depends on temperature: at 550 °C, the phenols concentration decreases in the presence of alanine, whereas at 460 and 500 °C, it is increased. In both cases, in the experiments with biomass and model compounds, an increase of the phenols concentration is found at 500 °C in the presence of protein and alanine, respectively. The phenols formation is not well-understood; therefore, it is difficult to explain why this temperature dependence occurs. In regard of the reaction scheme, a simple explanation would be that, if less gas is formed at 460 or 500 °C, the concentration of the short intermediates (Scheme 1) is higher, and therefore, more phenols are produced from these intermediates. At higher temperatures, the concentration of the short intermediates is low in any case; therefore, other effects may be important. In Part I, zoo mass was found to produce less formic acid.[65] This was not observed for the alanine addition. Formic acid is supposed to be an intermediate of the water gas shift reaction (see ref 57 and literature cited there), which is catalyzed by alkali salts. The different content of inorganic ingredients in the biomasses used and in the model systems might be the reason for the deviation. Not every difference between the experimental results with zoo mass and the phyto mass is a consequence of the Maillard reaction!

In Part I, it was shown that salts may compensate the effect of proteins and increase the gas yield if their concentration is high enough. This is confirmed in the batch experiments: adding salts to zoo mass increases the gas yield (Figure 9). The same effect is found for adding formaldehyde (Figure 9). This is not surprising: the effect of alkali salts is supposed to be a result of forming "active hydrogen".[57] Also, formaldehyde is a reducing agent and can be regarded as active hydrogen.

A characteristic feature of the batch reactor, in contrast to the tubular reactor and the CSTR, is the relatively high amount of coke formed. The reason is the relatively low heating rate (see refs 28 and 52). Therefore, the solid particles found contain much carbon not found in the particles described in Part I when reporting experiments in a CSTR. The particles of Type I are nearly pure coke particles. The particles of Type II with the relatively high Cr-oxide content are typical corrosion products. Interesting are particles of Type III, because they seem to contain

Scheme 3 . Reaction Pathways of Hydrothermal Biomass Degradation in the Presence of Proteins (Note: This scheme is based on a similar one developed by one of the unknown reviewers)

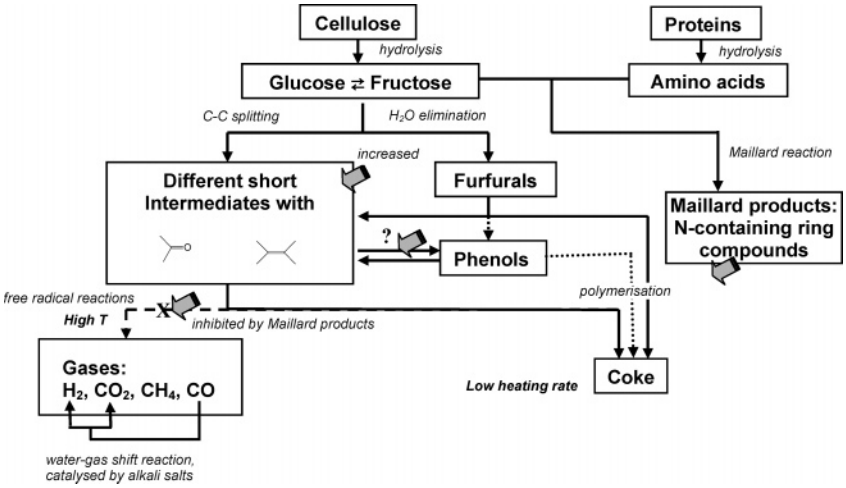

NiP. It is not clear so far where this comes from. Type IV particles seem to include NiS and organic compounds. This can be regarded as a hint: the sulfur reacts with the surface of the reactor as assumed in Part I.[65] On the other hand, no serious corrosion was observed as reported in Part I. Likely, the higher coke formation in the batch reactor protects the surface to a certain extent.

It is known that reactor materials may have a catalytic effect on gasification. Here, the additional experiments with the Inconel plate leads to the identical results. If there was a catalytic effect, the area of the plate was too small or the catalytic centers were poisoned fast, likely because of the high coke formation or because of poisoning by sulfur.

Conclusion

In the experiments with biomass, proteins reduce the gas yield and a higher DOC content is measured (Figure 9, part 1). In the model systems, the same effect occurs if the amino acid alanine is added to glucose. Glucose is a consecutive product of the carbohydrate degradation of biomass in supercritical water. Amino acids are consecutive products of the protein degradation (Scheme 3). Obviously these two reaction pathway may interfere (Scheme 3). It can be assumed the effect found for the presence of proteins or alanine is a result of the reaction of glucose or its consecutive products with amino acids or its consecutive products via the Maillard reaction (Figure 9). These types of reactions lead to nitrogen containing cyclic organic compounds, which are more or less strong free radical scavengers and inhibit free radical chain reactions. Their presence should reduce the formation of gases with a corresponding increase in the DOC value, because gases are produced mainly by free radical reactions (Scheme 3). Other types of reactions are less influenced, as can be seen from the only moderate effect on the key compounds discussed. So it is likely that the inhibition effect of proteins on biomass gasification and of alanine on glucose gasification is an outcome of forming nitrogen containing free radical scavengers. Salts can be used to compensate the effect.

Acknowledgment

The EPR-spectroscopy analysis done by Dr. Kamlowski from the company Bruker is gratefully acknowledged. The authors thank A. Böhm and K. Hedwig for analysis of the liquid- and gas-phase samples. Some experimental work was carried out by T. Tietz, who is thanked. Many thanks also to Mr. Schübel and Mr. Hager for the technical support. The authors would like to thank Mrs. Will and Dr. Jay for the GC-MS analysis as well as Mr. Habicht for the particle analysis. The authors thank also the unknown reviewers for improving this paper by their comments.

Literature Cited

(1) Modell, M. Gasification and Liquefaction of Forest Products in Supercritical Water. In *Fundamentals of Thermochemical Biomass Conversion*; Overend, R. P., Milne, T. A., Mudge, L. K., Eds.; Elsevier Applied Science Publisher: London and New York, 1985; p 95.

(2) Sealock, L. J.; Elliott, D. C.; Baker, E. G. Chemical Processing in High-Pressure Aqueous Environments. 3. Batch Reactor Process Development Experiments for Organics Destruction. *Ind. Eng. Chem. Res.* **1994**, *33*, 558.

(3) Yu, D.; Aihara, M.; Antal, M. J., Jr. Hydrogen Production by Steam Reforming Glucose in Supercritical Water. *Energy Fuels* **1993**, *7*, 574.

(4) Xu, X.; Matsumura, Y.; Stenberg, J.; Antal, M. J., Jr. Carbon-catalyzed Gasification of Organic Feedstocks in Supercritical Water. *Ind. Eng. Chem. Res.* **1996**, *35*, 2522.

(5) Xu, X.; Antal, M. J., Jr. Gasification of Sewage Sludge and other Biomass for Hydrogen Production in Supercritical Water. *Environ. Prog.* **1998**, *17*, 215.

(6) Goto, M.; Obuchi, R.; Hirose, T.; Sakaki, T.; Shibata, M. Hydrothermal conversion of municipal organic waste into resources. *Bioresour. Technol.* **2004**, *93*, 279.

(7) Goudriaan, F.; Peferoen, D. G. R. Liquid Fuels from Biomass via a Hydrothermal Process. *Chem. Eng. Sci.* **1990**, *45*, 2729.

(8) Haghighat Khajavi, S.; Kimura, Y.; Oomori, T.; Matsuno, R.; Adachi, S. Decomposition Kinetics of Maltose in Subcritical Water. *Biosci. Biotechnol. Biochem.* **2004**, *68*, 91.

(9) Jomaa, S.; Shanableh, A.; Khalil, W.; Trebilco, B. Hydrothermal Decomposition and Oxidation of the Organic Component of Municipal and Industrial Waste Products. *Adv. Environ. Res.* **2003**, *7*, 647.

(10) Minowa, T.; Murakami, M.; Dote, Y.; Ogi, T.; Yokoyama, S. Oil Production from Garbage by Thermochemical Liquefaction. *Biomass Bioenergy* **1995**, *8*, 117.

(11) Minowa, T.; Ogi, T. Hydrogen Production from Cellulose using a Reduced Nickel Catalyst. *Catal. Today* **1998**, *45*, 411.

(12) Minowa, T.; Zhen, F.; Ogi, T. Cellulose Decomposition in Hot-Compressed Water with Alkali or Nickel Catalyst. *J. Supercrit. Fluids* **1998**, *13*, 253.

(13) Minowa, T.; Inoue, S. Hydrogen Production from Biomass by Catalytic Gasification in Hot Compressed Water. *Renewable Energy* **1999**, *16*, 1114.

(14) Osada, T.; Sato, T.; Arai, K.; Watanabe, M. Adschiri, T. Low-Temperature Catalytic Gasification of Lignin and Cellulose with a Ruthenium Catalyst in Supercritical Water. *Energy Fuels* **2004**, *18*, 327.

(15) Sasaki, M.; Adschiri, T.; Arai, K. Kinetics of Cellulose Conversion at 25 MPa in Sub- and Supercritical Water. *AIChE J.* **2004**, *50*, 192.

(16) Oomori, T.; Khajavi, S. H.; Kimura, Y.; Adachi, S.; Matsuno, R. Hydrolysis of Disaccharides Containing Glucose Residue in Subcritical Water. *Biochem. Eng. J.* **2004**, *18*, 143.

(17) Park, K. C.; Tomiyasu, H. Gasification Reaction of Organic Compounds Catalyzed by RuO_2 in Supercritical Water. *Chem. Commun. (Cambridge, England)* **2003**, 694.

(18) Sasaki, M.; Adschiri, T.; Arai, K. Fractionation of Sugarcane Bagasse by Hydrothermal Treatment. *Bioresour. Technol.* **2003**, *86*, 301.

(19) Minowa, T.; Fang, Z. Hydrogen Production from Cellulose in Hot Compressed Water Using Reduced Nickel Catalyst: Product Distribution at Different Reaction Temperatures. *J. Chem. Eng. Jpn.* **1998**, *31*, 488.

(20) Sasaki, M.; Kabyemela, B.; Malaluan, R.; Hirose, S.; Takeda, N.; Adschiri, T.; Arai, K. Cellulose Hydrolysis in Subcritical and Supercritical Water. *J. Supercrit. Fluids* **1998**, *13*, 261.

(21) Sasaki, M.; Furusawa, M.; Minami, K.; Adschiri, T.; Arai, K. Kinetics and Mechanism of Cellobiose Hydrolysis and Retro-Aldol Condensation in Subcritical and Supercritical Water. *Ind. Eng. Chem. Res.* **2002**, *41*, 6642.

(22) Sakanishi, K.; Ikeyama, N.; Sakaki, T.; Shibata, M.; Miki, T. Comparison of the Hydrothermal Decomposition Reactivities of Chitin and Cellulose. *Ind. Eng. Chem. Res.* **1999**, *38*, 2177.

(23) Kabyemela, B. M.; Adschiri, T.; Malaluan, R. M.; Arai, K.; Ohzeki, H. Rapid and Selective Conversion of Glucose to Erythrose in Supercritical Water. *Ind. Eng. Chem. Res.* **1997**, *36*, 5063.

(24) Schmieder, H.; Abeln, J.; Boukis, N.; Dinjus, E.; Kruse, A.; Kluth, M.; Petrich, G.; Sadri, E.; Schacht, M. Hydrothermal Gasification of Biomass and Organic Wastes. *J. Supercrit. Fluids* **2000**, *17*, 145.

(25) Kruse, A.; Gawlik, A. Biomass Conversion in Water at 330−410 °C and 30−50 MPa. Identification of Key Compounds for Indicating Different Chemical Reaction Pathways. *Ind. Eng. Chem. Res.* **2003**, *42*, 267.

(26) Kruse, A.; Henningsen, T.; Pfeiffer, J.; Sinag, A. Biomass Gasification in Supercritical Water; Influence of the Dry Matter Content and the Formation of Phenols. *Ind. Eng. Chem. Res.* **2003**, *42*, 3711.

(27) Sinag, A.; Kruse, A.; Schwarzkopf, V. Formation and Degradation Pathways of Intermediate Products Formed during the Hydropyrolysis of Glucose as a Model Substance for Wet Biomass in a Tubular Reactor. *Eng. Life Sci.* **2003**, *3*, 469.

(28) Sinag, A.; Kruse, A.; Rathert, J. Influence of the Heating Rate and the Type of Catalyst on the Formation of Selected Intermediates and on the Generation of Gases during Hydropyrolysis of Glucose with Supercritical Water in a Batch Reactor. *Ind. Eng. Chem. Res.* **2004**, *43*, 502.

(29) Sinag, A.; Kruse, A.; Schwarzkopf, V. Key compounds of the hydropyrolysis of glucose in supercritical water in the presence of K_2CO_3. *Ind. Eng. Chem. Res.* **2003**, *42*, 3516.

(30) Hao, X. H.; Guo, L. J.; Mao, X.; Zhang, X. M.; Chen, X. J. Hydrogen Production from Glucose used as a Model Compound of Biomass Gasified in Supercritical Water. *Int. J. Hydrogen Energy* **2003**, *28*, 55.

(31) Kabyemela, B. M.; Aschiri, T.; Malaluan, R. M.; Arai, K. Kinetics of Glucose Epimerization and Decomposition in Subcritical and Supercritical Water. *Ind. Eng. Chem. Res.* **1997**, *36*, 1552.

(32) D'Jesus, P.; Boukis, N.; Kraushaar-Czarnetzki, B.; Dinjus, E. Influence of Process Variables on Gasification of Corn Silage in Supercritical Water. *Ind. Eng. Chem. Res.* **2006**, *45*, 1622.

(33) D'Jesus, P.; Boukis, N.; Kraushaar-Czarnetzki, B.; Dinjus, E. Gasification of Corn and Clover Grass in Supercritical Water. *Fuel* **2006**, *85*, 1032.

(34) Elliott, D. C.; Hart, T. R.; Neuenschwander, G. G. Chemical Processing in High-Pressure Aqueous Environments. 8. Improved Catalysts for Hydrothermal Gasification. *Ind. Eng. Chem. Res.* **2006**, *45*, 3776.

(35) Karagöz, S.; Bhaskar, T.; Muto, A.; Sakata, Y. Hydrothermal Upgrading of Biomass: Effect of K_2CO_3 Concentration and Biomass/Water Ratio on Products Distribution. *Bioresour. Technol.* **2006**, *97*, 90.

(36) Kersten, S. R. A.; Potic, B.; Prins, W.; Van Swaaij, W. P. M. Gasification of Model Compounds and Wood in Hot Compressed Water. *Ind. Eng. Chem. Res.* **2006**, *45*, 4169.

(37) Lu, Y. J.; Guo, L. J.; Ji, C. M.; Zhang, X. M.; Hao, X. H.; Yan, Q. H. Hydrogen Production by Biomass Gasification in Supercritical Water: A Parametric Study. *Int. J. Hydrogen Energy* **2006**, *31*, 822.

(38) Matsumura, Y.; Yanachi, S.; Yoshida, T. Glucose Decomposition Kinetics in Water at 25 MPa in the Temperature Range of 448−673 K. *Ind. Eng. Chem. Res.* **2006**, *45*, 1875.

(39) Williams, P. T.; Onwudili, J. Subcritical and Supercritical Water Gasification of Cellulose, Starch, Glucose, and Biomass Waste. *Energy Fuels* **2006**, *20*, 1259.

(40) Yan, Q.; Guo, L.; Lu, Y. Thermodynamic Analysis of Hydrogen Production from Biomass Gasification in Supercritical Water. *Energy Convers. Manage.* **2006**, *47*, 1515.

(41) Ehara, K.; Takada, D.; Saka, S. GC-MS and IR Spectroscopic Analyses of the Lignin-Derived Products from Softwood and Hardwood Treated in Supercritical Water. *J. Wood Sci.* **2005**, *51*, 256.

(42) Ehara, K.; Saka, S. Decomposition Behavior of Cellulose in Supercritical Water, Subcritical Water, and their Combined Treatments. *J. Wood Sci.* **2005**, *51*, 148.

(43) Haghighat Khajavi, S.; Kimura, Y.; Oomori, T.; Matsuno, R.; Adachi, S. Kinetics on Sucrose Decomposition in Subcritical Water. *Food Sci. Technol.* **2005**, *38*, 297.

(44) Elliott, D. C.; Phelps, M. R.; Sealock, J. J.; Baker, E. G. Chemical Processing in High-Pressure Aqueous Environments. 4. Continuous-flow Reactor Process Development Experiments for Organics Destruction. *Ind. Eng. Chem. Res.* **1994**, *33*, 566.

(45) Antal, M. J.; Mok, W. S. L.; Richards, G. N. Mechanism of Formation of 5-(Hydroxymethyl)-2-furaldehyde from Fructose and Sucrose. *Carbohydr. Res.* **1990**, *199*, 91.

(46) Ando, H.; Sakaki, T.; Kohusho, T.; Shibata, M.; Uemura, Y.; Hatate, Y. Decomposition Behavior of Plant Biomass in Hot-Compressed Water. *Ind. Eng. Chem. Res.* **2000**, *39*, 3688.

(47) Antal, M. J.; Leesomboon, T.; Mok, W. S.; Richards, G. N. Mechanism of Formation of 2-Furaldehyde from Xylose. *Carbohydr. Res.* **1991**, *217*, 71.

(48) Antal, M. J.; Mok, W. S. L.; Richards, G. N. Four-carbon Model Compounds for the Reactions of Sugars in Water at High Temperature. *Carbohydr. Res.* **1990**, *199*, 111.

(49) Osada, M.; Sato, T.; Watanabe, M.; Aschiri, T.; Arai, K. Low-Temperature Catalytic Gasification of Lignin and Cellulose with a Ruthenium Catalyst in Supercritical Water. *Energy Fuels* **2004**, *18*, 327.

(50) Minowa, T.; Fang, Z.; Ogi, T.; Varhegyi, G. Decomposition of Cellulose and Glucose in Hot-Compressed Water under Catalyst-Free Conditions. *J. Chem. Eng. Jpn.* **1998**, *31*, 131.

(51) Yoshida, T.; Oshima, Y.; Matsumura, Y. Gasification of Biomass Model Compounds and Real Biomass in Supercritical Water. *Biomass Bioenergy* **2004**, *26*, 71.

(52) Fang, Z.; Minowa, T.; Smith, R. L., Jr.; Ogi, T.; Kozinski, J. A. Liquefaction and Gasification of Cellulose with Na_2CO_3 and Ni in Subcritical Water at 350 °C. *Ind. Eng. Chem. Res.* **2004**, *43*, 2454.

(53) Saka, S.; Ueno, T. Chemical Conversion of Various Celluloses to Glucose and its Derivatives in Supercritical Water. *Cellulose* **1999**, *6*, 177.

(54) Sasaki, M.; Goto, K.; Tajima, K.; Adschiri, T.; Arai, K. Rapid and Selective Retro-aldol Condensation of Glucose to Glycolaldehyde in Supercritical Water. *Green Chem.* **2002**, *4*, 285.

(55) Kabyemela, B. M.; Adschiri, T.; Malaluan, R. M.; Arai, K. Glucose and Fructose Decomposition in Subcritical and Supercritical water: Detailed Reaction Pathway, Mechanisms, and Kinetics. *Ind. Eng. Chem. Res.* **1999**, *38*, 2888.

(56) Matsumura, Y.; Minowa, T.; Potic, B.; Kersten, S. R. A.; Prins, W.; van Swaaij, W. P. M.; van de Beld, B.; Elliott, D. C.; Neuenschwander, G. G.; Kruse, A.; Antal, M. J., Jr. Biomass Gasification in Near- and Supercritical water: Status and Prospects. *Biomass Bioenergy* **2005**, *29*, 269.

(57) Kruse, A.; Dinjus, E. Influence of Salts During Hydrothermal Biomass Gasification: The Role of the Catalysed Water-Gas Shift Reaction. *Z. Phys. Chem. Neue Folge* **2005**, *219*, 341.

(58) Belsky, A. J.; Brill, T. B. Spectroscopy of Hydrothermal Reactions. 14. Kinetics of The pH-sensitve Aminoguanidin−Semicarbazide−Cyanate Reaction Network. *J. Phys. Chem. A* **1999**, *103*, 7829.

(59) Yoshida, Y.; Takahashi, Y.; Terashima, M. Simplified Reaction Model for Production of Oil, Amino Acids, and Organic Acids from Fish Meat by Hydrolysis under SubCritical and Supercritical Conditions. *J. Chem. Eng. Jpn.* **2004**, *36*, 599.

(60) Li, J.; Brill, T. B. Decarboxylation Mechanism of Amino Acids by Density Functional Theory. *J. Phys. Chem. A* **2003**, *107*, 5993.

(61) Li, J.; Brill, T. B. Spectroscopy of Hydrothermal Reactions 25: Kinetics of the Decarboxylation of Protein Amino Acids and the Effect of Side Chains on Hydrothermal Stability. *J. Phys. Chem. A* **2003**, *107*, 5987.

(62) Islam, M. N.; Kaneko, T.; Kobayashi, K. Reaction of Amino Acids in a Supercritical Water-Flow Reactor Simulating Submarine Hydrothermal Systems. *Bull. Chem. Soc. Jpn.* **2003**, *76*, 1171.

(63) Sato, N.; Quitain, A. T.; Kang, K.; Daimon, H.; Fujie, K. Reaction Kinetics of Amino Acid Decomposition in High-Temperature and High-Pressure Water. *Ind. Eng. Chem. Res.* **2004**, *43*, 3217.

(64) Faisal, M.; Sato, N.; Quitain, A. T.; Daimon, H.; Fujie, K. Hydrolysis and Cyclodehydration of Dipeptide under Hydrothermal Conditions. *Ind. Eng. Chem. Res.* **2005**, *44*, 5472.

(65) Kruse, A.; Krupka, A.; Schwarzkopf, V.; Gamard, C.; Henningsen, T. Influence of Proteins on the Hydrothermal Gasification and Liquefaction of Biomass. 1. Comparison of Different Feedstocks. *Ind. Eng. Chem. Res.* **2005**, *44*, 3013.

(66) Kruse, A.; Lietz, C. Measurement of Residence Time Distribution in Hot Compressed Water—First Results Obtained in a Helical Tube. *Chem. Eng. Technol.* **2003**, *26*, 1119.

(67) Kruse, A.; Meier, D.; Rimbrecht, P.; Schacht, M. Gasification of Pyrocatechol in Supercritical Water in the Presence of Potassium Hydroxide. *Ind. Eng. Chem. Res.* **2000**, *39*, 4842.

(68) Boukis, N.; Habicht, W.; Franz, G.; Dinjus, E. Behavior of Ni-base Alloy 625 in Methanol-Supercritical Water Systems. *Mater. Corros.* **2003**, *54*, 326.

(69) Habicht, W.; Boukis, N.; Franz, G.; Walter, O.; Dinjus, E. Exploring Hydrothermally Grown Potassium Titanate Fibers by STEM-in-SEM/EDX and XRD. *Microsc. Microanal.* **2006**, *12*, 322.

(70) Habicht, W.; Boukis, N.; Franz, G.; Dinjus, E. Investigation of Nickel-Based Alloys Exposed to Supercritical Water Environments. *Microchim. Acta* **2004**, *145*, 57.

(71) Kamlowski, A. ELEXSYS—Measurements conducted at Bruker Biospin: Germany, 2005.

(72) Jing, H.; Kitts, D. D. Comparison of the Antioxidative and Cytotoxic Properties of Glucose−Lysine and Fructose−Lysine Maillard reaction products. *Food Res. Int.* **2000**, *33*, 509.

(73) Morales, F. J.; Jimenez-Perez, S. Free Radical Scavenging Capacity of Maillard Reaction Products as Related to Colour and Fluorescence. *Food Chem.* **2001**, *72*, 119.

(74) Alaiz, M.; Zandbergen, H. W.; Hidalgo, F. J. Antioxidative Activity of Pyrrole, Imidazole, Dihydropyridine, and Pyridinium Salt Derivatives Produced in Oxidized Lipid/Amino Acid Browning Reactions. *J. Agric. Food Chem.* **1996**, *44*, 686.

(75) Rizzi, G. P. Free radicals in the Maillard reaction. *Food Rev. Int.* **2003**, *19*, 375.

Received for review August 9, 2006
Revised manuscript received October 16, 2006
Accepted October 19, 2006

IE061047H